

Performance Analysis for Unicast and Multicast Traffic in Broadcast-and-Select WDM Networks

Wen-Yu Tseng, Chuan-Ching Sue, and Sy-Yen Kuo[†]

Department of Electrical Engineering, National Taiwan University, Taipei, Taiwan
sykuo@cc.ee.ntu.edu.tw

Abstract

This paper presents the analysis of multicasting performance in broadcast-and-select wavelength division multiplexing (WDM) networks from two aspects: multicast session length and multicast group size. The protocol analyzed in this paper is based on an existing protocol which can schedule unicast and multicast traffic. The packet distance, determined by the Euclidean distance of session length and the group size of a multicast packet, is compared with the multicast distance to select the most appropriate scheduling method for multicast packets. Further comparisons on channel utilization and packet delay show that the session length will affect the channel dominance significantly and the group size will determine the range of multicast distance such that the performances will remain the same. In addition, multicast traffic with larger mean session length or mean group size will make some specific scheduling strategies fail to achieve optimal performance. If the multicast distance is properly chosen, performance tradeoffs can be made under the multicasting environments with large session length or large group size.

1. Introduction

Accompanied with computer applications and communication services such as distributed data processing, broadcasting systems, and teleconferencing, broadcast-and-select WDM networks need to schedule unicast and multicast traffic [1,2,9-14]. The existing protocols, however, result in low channel utilization and large packet delay for unicast traffic and system channel dominance for multicast traffic. The reservation-based multicast protocol [10], for instance, result in severe system channel dominance under multicast traffic with large session length, and causes large packet delay. The pre-allocation-based multicast protocol [12], have to build a huge pre-allocation table with many multicast groups and large group size. Furthermore, the research in [14] claims that optimal scheduling for multicast traffic would be too time consuming and complicated under the multicast traffic with large session length and group size.

In this paper we analyze the multicasting characteristics from two aspects: session length S and group size G . The scheduling protocol used in this paper is a combinational protocol, implementing the concept of *multicast distance* M_d to determine which scheduling method the multicast packet is based on [6].

The multicast distance M_d is defined to compare with the Euclidean distance of session length and group size. It could also be implemented on other multicast protocols easily. With M_d , the protocol combines the separate scheduling of unicast and multicast traffic (SS) and the scheduling of multicast traffic as unicast traffic (SMU) to achieve good channel utilization and small packet delay. There are two cases for the specific M_d . The protocol follows SS with $M_d = 0$, and follows SMU with $M_d \rightarrow \infty$. Multicasting environments with different session length S and group size G are discussed. S will have an effect on channel dominance for multicast traffic, and G will determine the value of M_d under performance tradeoffs. The performances of SS and SMU are also compared with each other.

2. Protocol and Analytic Model

2.1. Protocol

The proposed protocol originates from unicast-based protocols [5,6]. It is based on the pre-allocation method with FT-TR (Fixed Transmitter-Tunable Receiver) architecture. The protocol allocates one channel to node i as the home channel ε_i for the fixed transmitter, while the destination node tunes the receiver to ε_i to receive packets transmitted from node i . Because the network is a wavelength-limited system with $\Omega \leq N$, some nodes may be assigned to the same home channel and therefore, collisions need to be avoided.

In order to complete the transmission from the fixed transmitter of the source node to the tunable receiver of the destination node, an allocation map of data wavelength and tuning receiver wavelength is derived to determine the tuning wavelengths for Ω nodes at each time slot. The wavelength ϕ_i for the tunable receiver of node i at the time slot t is determined according to the following simple equation:

$$c_i = (i - t + 1) \bmod N \quad i = 0, 1, \dots, N - 1.$$

$$\phi_i = \begin{cases} \omega_{c_i} & 0 \leq c_i \leq \Omega - 1 \\ \phi & c_i \geq \Omega \end{cases}$$

$\phi_i = \phi$ means that the receiver is idle. As shown in Figure 1, each node is assigned Ω slots per cycle and idle for the remaining $N - \Omega$ slots. The cycle length is N time slots to achieve self-routing. However, the source node has to request the access privilege of the home channel to complete the transmission with the FT-TR architecture. The access requests of the home channels are collected through the control channel ω_Ω .

[†] **Acknowledgment:** This research was supported by the National Science Council, Taiwan, R. O. C., under the Grant NSC 87-2213-E259-007.

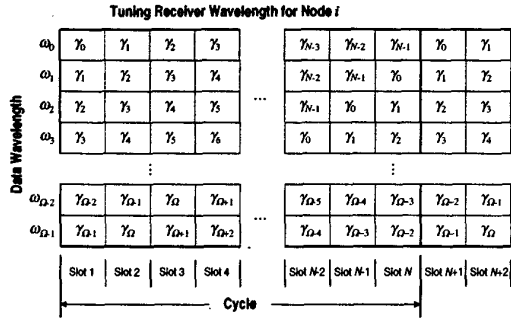


Figure 1. Data wavelength/tuning receiver wavelength allocation map for the combinational protocol.

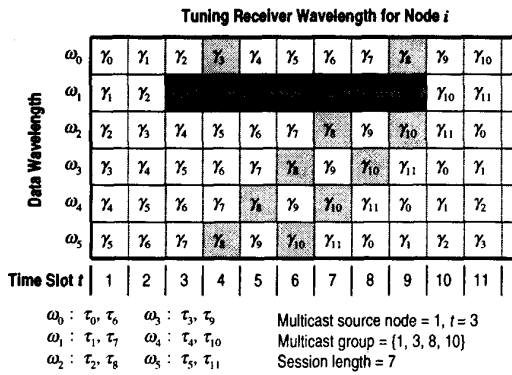


Figure 2. The MSR manipulates two qualified multicast packets at different time slots.

The Multicast Slot Reservation (MSR) employed in the protocol verifies the multicast packet, makes a reservation of the channel for the packet, and modifies the allocation map on each node. When the node receives a multicast packet with session length S and a multicast group G (with size G), the MSR examines first if the packet is qualified to make the reservation according to the packet distance M and the multicast distance M_d . If M is smaller than or equal to M_d , the packet is usually scheduled as a unicast packet. The MSR replicates the packet and transmits the replicated packets from the multicast source node to members of the multicast group respectively. If M is larger than M_d , the packet is scheduled as a multicast packet. Then the MSR makes the reservation of the home channel for the multicast source node. The number of time slots reserved for the packet is equal to S .

After reserving the home channel, the MSR examines the receiver availability of the multicast group and deletes the slots pre-allocated for the receivers in the multicast group during the multicast session. The slots pre-allocated for the receivers not included in the multicast group still follow the original unicast-based protocol. As shown in Figure 2, for instance, the MSR manipulates two qualified multicast packets at different time slots. For the packet at the time slot 3, the MSR reserves ω_1 from the time slot 3 to the time slot 9 as shown in the gradient area. Then the MSR deletes 10 slots as shown in the shaded areas during the multicast session from the time slot 3 to the time slot 9. This means that no other transmissions to the receivers

of nodes 3, 8, and 10 could be accomplished during the multicast session. The detailed algorithm is shown in [6].

2.2. Analytic model

Multicast traffic can be modeled with the multicast session length S and the multicast group G , while the size of the multicast group is denoted as G . The random variable S in the given multicast packet has the modified geometric distribution with the mean session length s , and the probability of a multicast packet with the session length k is

$$\text{Prob}(S = k) = \begin{cases} \frac{1}{s} \left(1 - \frac{1}{s}\right)^{k-1}, & k \geq 1 \\ 0, & \text{otherwise} \end{cases} \quad (1)$$

S is obviously no less than 1, and assumed to be no larger than N in order to maintain the allocation map and to support the protocol.

The size G of the multicast group in the given multicast packet follows the modified binomial distribution with the mean size $g \cdot (N - 3) + 2$, and the probability of a multicast packet with $G = l$ is

$$\text{Prob}(G = l) = \begin{cases} \binom{N-3}{l-2} \cdot g^{l-2} \cdot (1-g)^{N-l-1}, & 2 \leq l \leq N-1 \\ 0, & \text{otherwise} \end{cases} \quad (2)$$

Where g is the Bernouli probability that a destination node belongs to the multicast group. Because a multicast group contains at least two destination nodes, G is no less than 2 and no larger than $N - 1$.

Apart from the discussion of multicast traffic in [12], we define the *multicast distance* M_d to determine the scheduling strategies for multicast traffic. Let the packet distance M be the Euclidean distance between S and G ; that is,

$$M = \sqrt{S^2 + G^2}. \quad (3)$$

Each multicast packet has its own value of M . The protocol compares M with M_d and determines the scheduling strategies. There are two cases for the specific M_d . The protocol follows SS when $M_d = 0$, and follows SMU when $M_d \rightarrow \infty$.

When $0 < M_d < \infty$, the M_d curve is shown in Figure 3 to compare M with M_d . The probability of $M \leq M_d$, inside the shaded curve as shown in Figure 3, can be denoted as F :

$$F = \text{Pr}(M \leq M_d) = \text{Pr}\left(\sqrt{S^2 + G^2} \leq M_d\right) \\ = \sum_{k=1}^{\lfloor M_d-1 \rfloor} \left[\sum_{l=2}^{\lfloor \sqrt{M_d^2 - k^2} \rfloor} \text{Pr}(S = k) \cdot \text{Pr}(G = l) \right]. \quad (4)$$

Transmitting such packet need not occupy a specific channel for a long time, and only a few receivers have to be reserved. Therefore the packet is scheduled in a way similar to SMU. That is, the protocol replicates the packet to transmit from the multicast source node to members of the multicast group.

The probability of $M > M_d$, outside the shaded curve as shown in Figure 3, can be denoted as $1 - F$. Transmitting such

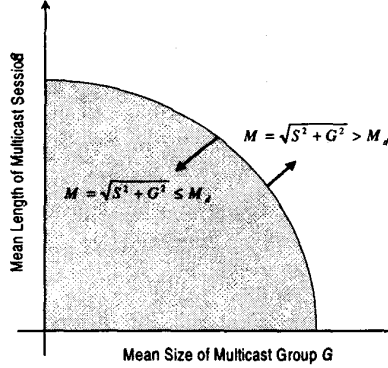


Figure 3. The multicast distance curve to determine the scheduling strategies for multicast traffic.

packet will occupy a specific channel for a long time, and a lot of receivers are reserved. If SMU is adopted, the number of packets in the unicast queues will be increased rapidly, and the unicast packet delay is increased dramatically. Therefore the packet is scheduled in a way similar to SS. The protocol immediately performs the MSR to reserve the system channel and the receivers in the multicast group. Although the reserved channel and the receivers are dominated by multicast traffic, the performance degradation induced is far less than that with SMU.

The analytic model analyzes the influences on session length and group size under multicast traffic. The assumptions for the model are described as follows:

1. All nodes are assumed to behave independently.
2. A packet arriving at node i , $0 \leq i \leq N-1$, follows the Poisson arrival process, with an arrival rate of ρ packets per unit time slot per node.
3. The packet arriving at node i is a multicast packet with probability q , and a unicast packet with probability $1-q$.
4. If the packet arriving at node i is a unicast packet, it is destined for node j with probability $\lambda = (N-1)^{-1}$ for $j \neq i$, $0 \leq j \leq N-1$, and 0 when $j = i$.
5. If the packet arriving at node i is a multicast packet, the session length S and the multicast group size G follow the probability distributions described above. The members of the multicast group G are randomly chosen with uniform probability $\rho = G/(N-1)$ for $i \in G$.
6. At most one new packet can arrive at a node per time slot.
7. Each queue has the capacity to hold B packets, including the one currently being processed by the transmitter.

The four possible states of the queues are *unicast* state $S_{u,i}$ — transmitting unicast packets, *unicast wait* state $S_{uw,i}$ — waiting after transmitting the unicast packet until the next cycle to transmit arrives, *multicast* state $S_{m,i}$ — transmitting multicast packets, and *multicast wait* state $S_{mw,i}$ — waiting after transmitting the multicast packet until the next slot to transmit arrives, $0 \leq i \leq B$. $S_{u,i}$ and $S_{mw,i}$ are determined by the number of unicast packets in the unicast queue and the unicast packet at the head of the unicast queue. $S_{m,i}$ and $S_{mw,i}$ are also determined by the number of unicast packets in the queue. The arrivals of multicast packets are indicated as the multicast status of the node.

The packet arrival rate and sojourn time of state $S_{x,i}$, $x \in \{u, uw, m, mw\}$, are defined as follows. The sojourn time of

the state $S_{x,i}$ is $\tau_{x,i}$. No packet arrives at state $S_{x,i}$ with probability $\alpha_{x,i} = e^{-\rho\lambda\tau_{x,i}}$. A new unicast packet arrives at state $S_{x,i}$ with probability $\beta_{x,i} = (1-q) \cdot (1 - e^{-\rho\lambda\tau_{x,i}})$. If $\tau_{x,i} > 1$, the number of packet arrivals can be larger than 1. Thus $\beta_{x,i} = (1-q) \cdot \sum_{n=1}^{\infty} P_{x,i}(n) = (1-q) \cdot \sum_{n=1}^{\infty} \frac{1}{n!} \cdot e^{-\rho\lambda\tau_{x,i}} \cdot (\rho\lambda\tau_{x,i})^n$. A new multicast packet arrives with probability $\gamma_{x,i} = q \cdot (1 - e^{-\rho\lambda\tau_{x,i}})$. It is obvious that $\alpha_{x,i} + \beta_{x,i} + \tau_{x,i} = 1$. In order to model that a multicast packet is replicated to the unicast packets, the probability of $S = k$ with $M \leq M_d$ is

$$P_F(k) = \Pr(S = k, M \leq M_d) = \Pr(S = k, \sqrt{S^2 + G^2} \leq M_d)$$

$$= \sum_{l=2}^{\lfloor \sqrt{M_d^2 - k^2} \rfloor} \Pr(S = k) \cdot \Pr(G = l). \quad (5)$$

Based on the idea of arrival of the multicast packet as the multicast status of the node, the semi-Markov analytic model of the combinational protocol can be derived. The limiting probabilities of being in $S_{x,i}$, denoted as $v_{x,i}$, can be obtained by solving steady-state equations. The steady-state equations for $S_{u,i}$ are shown below:

$$v_{u,0} = v_{u,0}[\alpha_{u,0} + (1-\rho)\gamma_{u,0}F] + v_{u,1}[\alpha_{u,1} + (1-\rho)\gamma_{u,1}F] + v_{m,0}[\alpha_{m,0} + (1-\rho)\gamma_{m,0}F]. \quad (6)$$

$$v_{u,1} = v_{uw,0}\zeta[\alpha_{uw,0} + (1-\rho)\gamma_{uw,0}F] + v_{uw,1}\zeta[\alpha_{uw,1} + (1-\rho)\gamma_{uw,1}F]. \quad (7)$$

$$v_{u,i} = v_{uw,0}\zeta[\rho\gamma_{uw,0}P_F(i-1) + P_{uw,0}(i-1)] + v_{uw,i}\zeta[\alpha_{uw,i} + (1-\rho)\gamma_{uw,i}F] + \sum_{j=1}^{i-1} v_{uw,j}\zeta[\rho\gamma_{uw,j}P_F(i-j) + P_F(i-j)], \quad 2 \leq i \leq B-1. \quad (8)$$

$$v_{u,B} = v_{uw,0}\zeta\left[\rho\gamma_{uw,0}\sum_{k=B-1}^{\infty} P_F(k) + \beta_{uw,0} - \sum_{j=1}^{B-2} P_{uw,0}(j)\right] + \sum_{i=1}^{B-1} v_{uw,i}\zeta\left[\rho\gamma_{uw,i}\sum_{k=B-i}^{\infty} P_F(k) + \beta_{uw,i} - \sum_{j=1}^{B-i-1} P_{uw,i}(j)\right] + v_{uw,B}\zeta[\alpha_{uw,B} + \beta_{uw,B} + \gamma_{uw,B}F]. \quad (9)$$

Note that ζ is the probability that the node can access the channel. The transitions from $S_{uw,i}$ to $S_{u,i}$ may happen except $S_{u,0}$. $S_{u,0}$ is the special state which makes transitions from $S_{m,0}$, $S_{u,1}$ and $S_{u,0}$ itself. The steady-state equations for $S_{uw,i}$ are shown below:

$$v_{uw,0} = v_{u,0}[\beta_{u,0} + \rho\gamma_{u,0}P_F(1)] + v_{uw,0}(1-\zeta)[\alpha_{uw,0} + (1-\rho)\gamma_{uw,0}F] + v_{m,0}[\rho\gamma_{m,0}P_F(1) + P_{m,0}(1)] \quad (10)$$

$$v_{uw,i} = \sum_{j=0}^{i-1} v_{u,j}\rho\gamma_{u,j}P_F(i-j+1) + v_{u,i}[\beta_{u,i} + \rho\gamma_{u,i}P_F(1)] + v_{u,i+1}[\alpha_{u,i+1} + (1-\rho)\gamma_{u,i+1}F] + \sum_{j=0}^{i-1} v_{uw,j}(1-\zeta)[\rho\gamma_{uw,j}P_F(i-j) + P_{uw,j}(i-j)] + v_{uw,i}(1-\zeta)[\alpha_{uw,i} + (1-\rho)\gamma_{uw,i}F] + v_{m,0}[\rho\gamma_{m,0}P_F(i+1) + P_{m,0}(i+1)] + \sum_{j=1}^{i-1} v_{m,j}[\rho\gamma_{m,j}P_F(i-j) + P_{m,j}(i-j)]$$

$$+ v_{m,i} [\alpha_{m,i} + (1-\rho)\gamma_{m,i}F], \quad 1 \leq i \leq B-2. \quad (11)$$

$$\begin{aligned} v_{uw,B-1} &= \sum_{j=0}^{B-2} v_{u,j} \rho \gamma_{u,j} P_F(B-j) + v_{u,B-1} [\beta_{u,B-1} + \rho \gamma_{u,B-1} P_F(1)] \\ &+ v_{u,B} [\alpha_{u,B} + \beta_{u,B} + \gamma_{u,B} F] \\ &+ v_{uw,0} (1-\zeta) \left[\rho \gamma_{uw,0} \sum_{k=B-1}^{\infty} P_F(k) + \beta_{uw,0} - \sum_{j=1}^{B-2} P_{uw,0}(j) \right] \\ &+ \sum_{j=1}^{B-2} v_{uw,j} (1-\zeta) [\rho \gamma_{uw,j} P_F(B-j-1) + P_{uw,j}(B-j-1)] \\ &+ v_{uw,B-1} (1-\zeta) [\alpha_{uw,B-1} + (1-\rho)\gamma_{uw,B-1} F] \\ &+ v_{m,0} [\rho \gamma_{m,0} P_F(B) + P_{m,0}(B)] \\ &+ \sum_{j=1}^{B-2} v_{m,j} [\rho \gamma_{m,j} P_F(B-j-1) + P_{m,j}(B-j-1)] \\ &+ v_{m,B-1} [\alpha_{m,B-1} + (1-\rho)\gamma_{m,B-1} F]. \end{aligned} \quad (12)$$

$$\begin{aligned} v_{uw,B} &= \sum_{j=0}^{B-1} v_{u,j} \left[\rho \gamma_{u,j} \sum_{k=B-j+1}^{\infty} P_F(k) \right] + v_{m,B} [\alpha_{m,B} + \beta_{m,B} + \gamma_{m,B} F] \\ &+ v_{uw,B} (1-\zeta) [\alpha_{uw,B} + \beta_{uw,B} + \gamma_{uw,B} F] \\ &+ v_{m,0} \left[\rho \gamma_{m,0} \sum_{k=B+1}^{\infty} P_F(k) + \beta_{m,0} - \sum_{k=1}^B P_{m,0}(k) \right] \\ &+ \sum_{j=1}^{B-1} v_{m,j} \left[\rho \gamma_{m,j} \sum_{k=B-j}^{\infty} P_F(k) + \beta_{m,j} - \sum_{k=1}^{B-j-1} P_{m,j}(k) \right]. \end{aligned} \quad (13)$$

Note that the transitions from $S_{u,i}$, $S_{m,i}$ and $S_{uw,i}$ to $S_{uw,i}$ can occur with the probability described above. Only transitions from $S_{mw,i}$ to $S_{uw,i}$ can not occur because they are the waiting states. The steady-state equations for $S_{m,i}$ are shown below:

$$\begin{aligned} v_{m,0} &= v_{mw,0} [\alpha_{mw,0} + (1-\rho)\gamma_{mw,0}F + \gamma_{mw,0}F] \quad (14) \\ v_{m,i} &= v_{uw,0} [\gamma_{uw,0} (1-F) P_{uw,0}(i-1)] + \sum_{j=1}^i v_{uw,j} [\gamma_{uw,j} (1-F) P_{uw,j}(i-j)] \\ &+ \sum_{j=0}^{i-1} v_{mw,j} [\rho \gamma_{mw,j} P_F(i-j) + P_{mw,j}(i-j)] \\ &+ v_{mw,i} [\alpha_{mw,i} + (1-\rho)\gamma_{mw,i}F + \gamma_{mw,i}F], \quad 1 \leq i \leq B-1. \end{aligned} \quad (15)$$

$$\begin{aligned} v_{m,B} &= v_{uw,0} (1-F) \left[1 - \sum_{j=0}^{B-2} P_{uw,0}(j) \right] \\ &+ \sum_{j=1}^{B-1} v_{uw,j} \gamma_{uw,j} (1-F) \left[1 - \sum_{k=0}^{B-j-1} P_{uw,j}(k) \right] + v_{uw,B} \gamma_{uw,B} (1-F) \\ &+ \sum_{j=0}^{B-1} v_{mw,j} \left[\rho \gamma_{mw,j} \sum_{k=B-j}^{\infty} P_F(k) + \beta_{mw,j} - \sum_{k=1}^{B-j-1} P_{mw,j}(k) \right]. \end{aligned} \quad (16)$$

Note that the transitions from $S_{uw,i}$ and $S_{mw,i}$ to $S_{m,i}$ can occur with the probability described above. The steady-state equations for $S_{mw,i}$ are derived as

$$v_{mw,0} = v_{u,0} \gamma_{u,0} (1-F) + v_{u,1} \gamma_{u,1} (1-F) + v_{m,0} \gamma_{m,0} (1-F). \quad (17)$$

$$v_{mw,i} = v_{u,i+1} \gamma_{u,i+1} (1-F) + v_{m,i} \gamma_{m,i} (1-F), \quad 1 \leq i \leq B-1. \quad (18)$$

$$v_{mw,B} = v_{m,B} \gamma_{m,B} (1-F). \quad (19)$$

3. Performance Analysis: Group Size

Three performance metrics are discussed. Channel utilization for unicast traffic (U_u) is defined as the number of channels used

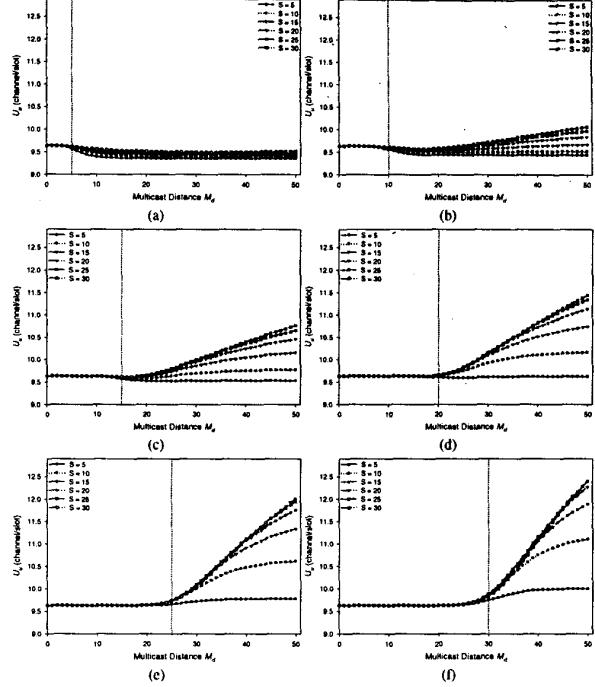


Figure 4. U_u vs. M_d : (a) $G = 5$, (b) $G = 10$, (c) $G = 15$, (d) $G = 20$, (e) $G = 25$, and (f) $G = 30$.

by unicast traffic per time slot. U_u reveals the variations of unicast transmissions on the protocols for multicast traffic. Channel utilization for multicast traffic (U_m) is defined as the number of channels used by multicast traffic per time slot. U_m reveals the channel dominance for multicast traffic. Packet delay for unicast traffic (D_u) is the number of time slots taken from the time slot that a unicast packet is generated at the source node to the time slot that the packet is received at the destination node. D_u reveals the efficiency of the network which schedules the unicast and multicast traffic. Packet delay for multicast traffic (D_m) with $M > M_d$ is almost 0 because the protocol preemptively schedules the multicast packet.

In this section, the metrics are analyzed with fixed group size and variable session lengths. The parameters in the model are described as follows: $N = 100$ network nodes, $\Omega = 40$ data wavelengths. The buffer size of the queue is $B = 50$. The packet generation rate is $p = 0.1$ and the multicast ratio is $q = 0.1$. The multicast distance M_d is a variable to analyze the performance metrics. The session length varies from 5 to 30 with an increment of 5. The group size also varies from 5 to 30 with an increment of 5. The purpose of the analysis in this section is to understand the effect of the group size on the multicast traffic.

3.1. Channel utilization for unicast traffic U_u

Comparisons on channel utilization for unicast traffic U_u with fixed group size are shown in Figure 4. With $G = 5$ as shown in Figure 4(a), U_u remains constant with $M_d < G$ and independent of S . In this case the probability that the protocol will schedule the multicast packets with SMU is very small. With $M_d \geq G$, U_u slightly decreases as M_d increases. In this case,

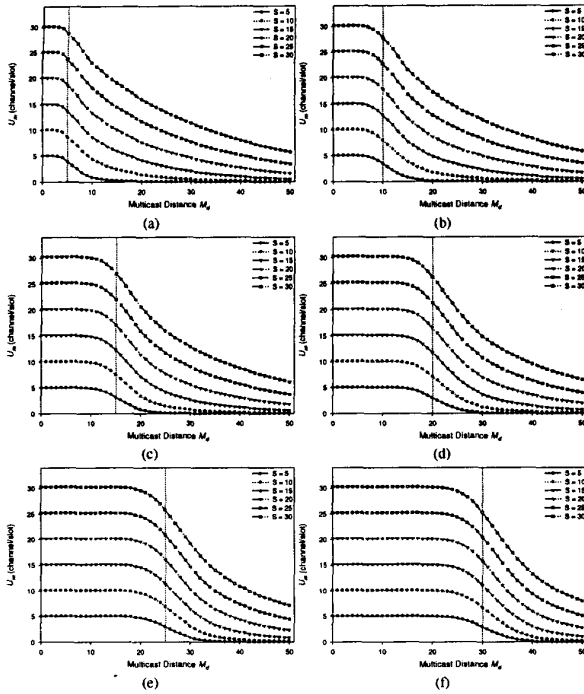


Figure 5. U_m vs. M_d : (a) $G = 5$, (b) $G = 10$, (c) $G = 15$, (d) $G = 20$, (e) $G = 25$, and (f) $G = 30$.

the probability that the protocol will schedule the multicast packets with SMU increases. Because the group size is too small, the protocol makes unicast traffic load with $M_d \geq G$ slightly lower than that with $M_d = 0$ (SS). The effect induced by S is not significant.

With $G = 10, 15, \dots, 30$, as shown in Figure 4(b)-(f), the curves for U_u are different from that with $G = 5$. U_u remains the same with $M_d < G$ no matter what the value of S is. Same as $G = 5$, the probability that the protocol will schedule the multicast packets with SMU is very small. With $M_d \geq G$, U_u increases as M_d increases. In addition, U_u also increases as S increases because the protocol makes unicast traffic load with $M_d \geq G$ proportional to S and larger than that with SS. When $M_d \rightarrow \infty$ (SMU) and all multicast packets are scheduled as unicast packets, the number of unicast packets increases indefinitely. However, with $G = 25$ and 30 , U_u saturates gradually with large S . Therefore, the impact of U_u is clearly related to the value of the group size.

3.2. Channel utilization for multicast traffic U_m

Comparisons on channel utilization for multicast traffic U_m with fixed group size are shown in Figure 5. Because the number of time slots reserved for the multicast packet is large with large S , the probability of reserving the channel for the unicast transmission tends to be smaller. In addition, the number of multicast transmissions with different channels at the same time slot also increases as S increases. In Figure 5, U_m is proportional to S with $M_d = 0$ (SS) no matter what the value of G is. That is, the effect of channel dominance for multicast traffic is very evident as S increases.

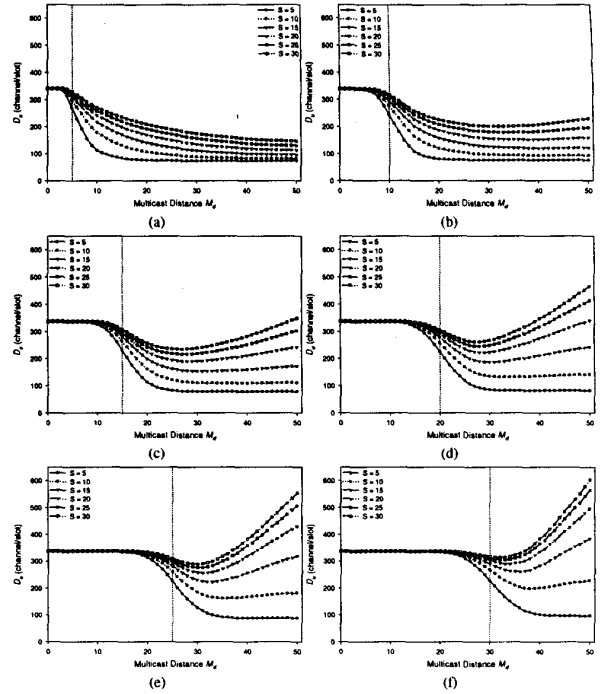


Figure 6. D_u vs. M_d : (a) $G = 5$, (b) $G = 10$, (c) $G = 15$, (d) $G = 20$, (e) $G = 25$, and (f) $G = 30$.

U_m remains almost unchanged with $M_d < G$. In this case the protocol schedules the multicast packets with SS. With $M_d \geq G$, U_m decreases as M_d increases; in addition, U_m approaches 0 with $M_d \rightarrow \infty$ (SMU). Because most of the multicast packets are scheduled as unicast packets with SMU and only a small number of multicast packets are scheduled with SS, the probability of the channel reserved for multicast transmission is reduced according to the value of M_d .

3.3. Packet delay for unicast traffic D_u

Comparisons on packet delay for unicast traffic D_u with fixed group size are shown in Figure 6. With $M_d = 0$ (SS), the value of D_u is constant no matter what the values of S and G are. Because the number of packets in the unicast queue does not change with S and G as well as U_u also remains constant, D_u remains constant according to the Little's law. D_u remains almost the same with $M_d < G$ because the probability that the protocol schedules the multicast packets with SMU is very small.

With $M_d \geq G$, D_u varies with different values of S and G . With $G = 5$ and 10 , D_u decreases as M_d increases. D_u decreases slightly with large S . This shows that SMU results in smaller D_u than other scheduling protocols as long as the group size is small. However, D_u varies with $G = 15, \dots, 30$. If $S < 15$, D_u decreases as M_d increases. Same with $G = 5$, SMU results in smaller D_u with very small session length. If $S \geq 15$, a minimal value of D_u is reached and D_u increases dramatically as M_d increases. The occurrence of the minimal D_u indicates that the protocol makes good partitions of multicast traffic for SS and SMU. The value of M_d with minimal D_u also induces smaller U_m and better U_u . Besides, the minimal D_u also minimizes the

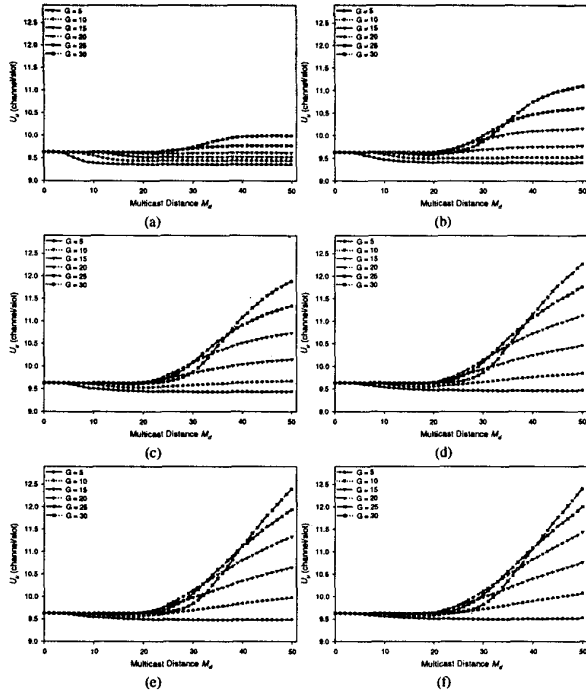


Figure 7. U_u vs. M_d : (a) $S = 5$, (b) $S = 10$, (c) $S = 15$, (d) $S = 20$, (e) $S = 25$, and (f) $S = 30$.

transmission time of the multicast packet with $M < M_d$, which is the session length times D_u . This means that the combinational protocol provides good performance tradeoffs with large S and G .

4. Performance Analysis: Session Length

In this section, the metrics are analyzed with fixed session length and variable group sizes. The group size varies from 5 to 30 with an increment of 5. Although the session length is fixed inside each figure, there are also 6 values from 5 to 30 with an increment of 5. The purpose of analysis in this section is to understand the effect of the session length on the multicast traffic.

4.1. Channel utilization for unicast traffic U_u

Comparisons on channel utilization for unicast traffic U_u with fixed session length are shown in Figure 7. With $M_d = 0$ (SS), U_u remains constant no matter what the value of G is. As M_d increases, U_u starts to increase from a specific M_d . Note that some curves are overlapped because the specific point is determined by the group size G . With $M_d \rightarrow \infty$ (SMU), U_u is determined straightforwardly by the session length S and the group size G . With $S = 5$ and 10, as shown respectively in Figure 7(a) and (b), the increase of U_u is limited by S , although U_u increases as G increases. Under such environments the probability that the protocol schedules the multicast packets with SMU is very small. With $S = 15, 20, 25$, and 30, the increase of U_u is proportional to G . For these cases the probability that the protocol schedules the multicast packets with SMU increases based on

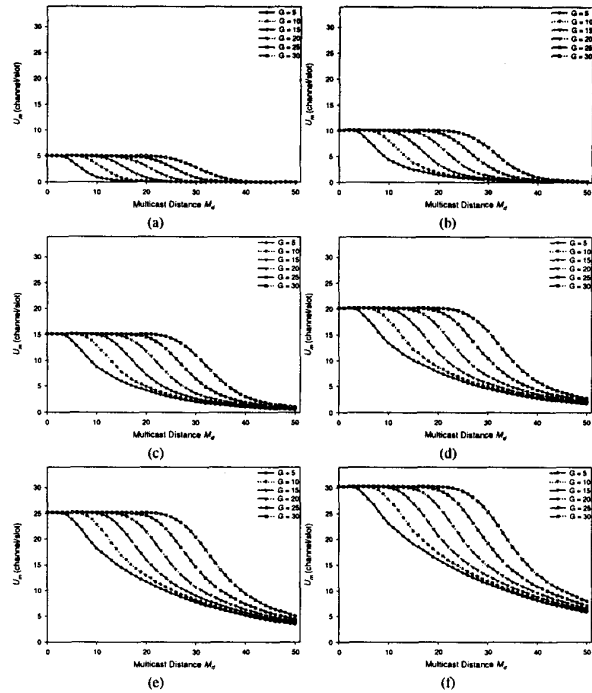


Figure 8. U_m vs. M_d : (a) $S = 5$, (b) $S = 10$, (c) $S = 15$, (d) $S = 20$, (e) $S = 25$, and (f) $S = 30$.

the group size G . Thus under the case with large session length, U_u will increase to the specific value according to the group size.

4.2. Channel utilization for multicast traffic U_m

Comparisons on channel utilization for multicast traffic U_m with fixed session length are shown in Figure 8. With $M_d = 0$ (SS), note that U_m is proportional to S no matter what G is. This is verified again that the effect of channel dominance for multicast traffic is very evident as S increases. As M_d increases, U_m does not decrease until M_d is larger than a specific value. This value is proportional to G . For the value of M_d that induces $F \cong 0.5$, U_m will decrease to $0.5U_m$ and $M_d \cong G$. With $M_d \rightarrow \infty$ (SMU), U_m approaches 0 theoretically. With $S = 25$ and 30, however, U_m decreases to the value other than 0 because the range of M_d used here is only from 0 to 50. This means that M_d has to be very large to suppress U_m to 0 if the session length is quite large. Therefore, the channel dominance for multicast traffic is significantly dependent on S .

4.3. Packet delay for unicast traffic D_u

Comparisons on packet delay for unicast traffic D_u with fixed session length are shown in Figure 9. With $M_d = 0$ (SS), the value of D_u is constant no matter what the values of S and G are. Because the number of packets in the unicast queue does not change with S and G , and U_u also remains constant, D_u remains constant according to the Little's law. D_u remains the same with $M_d < G$ because the probability that the protocol schedules the multicast packets with SMU is very small.

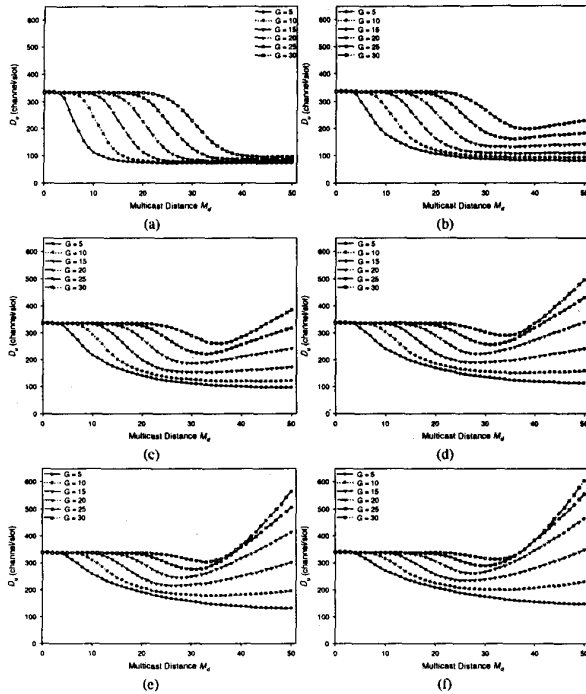


Figure 9. D_u vs. M_d : (a) $S = 5$, (b) $S = 10$, (c) $S = 15$, (d) $S = 20$, (e) $S = 25$, and (f) $S = 30$.

As M_d increases, D_u varies with different values of S and G . With $S = 5$ and 10 , D_u becomes smaller when M_d increases. D_u decreases slightly with large G . This shows that SMU results in smaller D_u than other scheduling protocols as long as the session length is very small. However, D_u varies with $S = 15, \dots, 30$. If $G < 15$, D_u decreases as M_d increases. Same with $S = 5$, SMU results in smaller D_u with very small group size. If $G \geq 15$, a minimal value of D_u is reached, and then D_u increases dramatically as M_d increases. A minimal value of D_u is reached and D_u increases dramatically as M_d increases. The occurrence of the minimal D_u indicates that the protocol makes good partitions of multicast traffic for SS and SMU. The value of M_d with the minimal D_u also induces smaller U_m and good U_u . Besides, the minimal D_u also minimizes the transmission time of the multicast packet with $M < M_d$, which is the session length times D_u . This means that the combinational protocol provides good performance tradeoffs with large S and G .

5. Conclusions

This paper analyzed the characteristics of multicast traffic for scheduling unicast and multicast traffic in broadcast-and-select WDM networks by examining the channel dominance and the packet delay. Different multicast scheduling strategies are compared with equivalent M_d . A semi-Markov model for performance analysis was described for the protocols. The model characterizes the arrival of the multicast packets as the multicast status in the queue, which reduces the state space of the model. The model was shown to accurately estimate the behavior of the multicasting protocols.

The channel utilization for unicast traffic U_u , the channel utilization for multicast traffic U_m , and the packet delay for unicast traffic D_u were studied with variations on the multicast distance in the broadcast-and-select WDM networks. The experiments compared different values of M_d in order to map the other two scheduling strategies. SS, representing $M_d = 0$, results in significant channel dominance for multicast traffic. Although SMU, representing $M_d \rightarrow \infty$, suppresses U_m to 0 to eliminate the channel dominance for multicast traffic totally, it results in very large D_u . As long as the value of M_d for minimal D_u is selected, U_u will be slightly increased and U_m will be significantly reduced. Therefore, performance tradeoffs between SS and SMU, provided by the combinational protocol with the use of M_d , can be made under the multicasting environments with large session length or large group size.

References

- [1] J. S. Turner, "The Challenge of Multipoint Communication," in *Proceedings of 5th ITC Seminar*, pp. 263-279, May 1987.
- [2] M. Ammar, G. Polyzos, and S. Tripathi (Eds.), Special Issue on Network Support for Multipoint Communication, *IEEE J. Select. Areas Commun.*, vol. 15, no. 3, Apr. 1997.
- [3] B. Mukherjee, "WDM-Based Local Lightwave Networks Part I: Single-Hop Systems," *IEEE Network Mag.*, pp. 12-27, May 1992.
- [4] K. M. Sivalingam, K. Bogineni, and P. W. Dowd, "Pre-Allocation Media Access Control Protocols for Multiple Access WDM Photonic Networks," *ACM SIGCOMM'92*, pp. 235-246, Aug. 1992.
- [5] K. Bogineni, K. M. Sivalingam, and P. W. Dowd, "Low-Complexity Multiple Access Protocols for Wavelength-Division Multiplexed Photonic Networks," *IEEE J. Select. Areas Commun.*, vol. 11, pp. 590-604, May 1993.
- [6] W. Y. Tseng and S. Y. Kuo, "A Combinational Media Access Protocol for Multicast Traffic in Single-Hop WDM LANs," *GLOBECOM'98*, pp. 294-299, Nov. 1998.
- [7] R. Chipalkatti, Z. Zhang, and A. S. Acampora, "Protocols for Optical Star-Coupler Network Using WDM: Performance and Complexity Study," *IEEE J. Select. Areas Commun.*, vol. 11, pp. 579-589, May 1993.
- [8] P. A. Humblet, R. Ramaswami, and K. N. Sivarajan, "An Efficient Communication Protocol for High-Speed Packet-Switched Multichannel Networks," *IEEE J. Select. Areas Commun.*, vol. 11, pp. 568-578, May 1993.
- [9] M. S. Borella and B. Mukherjee, "Efficient Scheduling of Nonuniform Packet Traffic in a WDM/TDM Local Lightwave Network with Arbitrary Transceiver Tuning Latencies," *IEEE J. Select. Areas Commun.*, vol. 14, no. 5, pp. 923-934, June 1996.
- [10] M. S. Borella and B. Mukherjee, "A Reservation-Based Multicasting Protocol for WDM Local Lightwave Networks," *ICC'95*, pp. 1277-1281, 1995.
- [11] J. P. Jue and B. Mukherjee, "The Advantages of Partitioning Multicast Transmissions in a Single-Hop Optical WDM Network," *ICC'97*, pp. 427-431, 1997.
- [12] G. N. Rouskas and M. H. Ammar, "Multidestination Communication Over Tunable-Receiver Single-Hop WDM Networks," *IEEE J. Select. Areas Commun.*, vol. 15, no. 3, pp. 501-511, Apr. 1997.
- [13] Z. Ortiz, G. N. Rouskas, and H. G. Perros, "Scheduling of Multicast Traffic in Tunable-Receiver WDM Networks with Non-Negligible Tuning Latencies," *ACM SIGCOMM'97*, Cannes, France, Sep. 1997.
- [14] E. Modiano, "Unscheduled Multicasts in WDM Broadcast-and-Select Networks," *INFOCOM'98*, 1998.
- [15] L. Sahasrabudhe and B. Mukherjee, "Probability Distribution of the Receiver Busy Time in a Multicasting Local Lightwave Network," *ICC'97*, pp. 116-120, 1997.